

1 **Mitochondrial oxidative stress drives IL-12/IL-18-induced**  
2 **IFN- $\gamma$  production by CD4<sup>+</sup> T cells and is controlled by Fas**

3 Gorjana Rackov<sup>1\*</sup>, Parinaz Tavakoli Zaniani<sup>1</sup>, Sara Colomo del Pino<sup>1</sup>, Rahman  
4 Shokri<sup>1#</sup>, Melchor Alvarez-Mon<sup>2,3</sup>, Carlos Martinez-A<sup>1</sup> and Dimitrios Balomenos<sup>1\*</sup>

5 <sup>1</sup>Department of Immunology and Oncology, Centro Nacional de Biotecnología-  
6 Consejo Superior de Investigaciones Científicas (CNB-CSIC), Madrid, Spain

7 <sup>2</sup> Service of Internal Medicine and Immune System Diseases-Rheumatology, University  
8 Hospital Príncipe de Asturias, (CIBEREHD), Alcalá de Henares, Spain.

9 <sup>3</sup>Department of Medicine and Medical Specialties, Faculty of Medicine and Health  
10 Sciences, University of Alcalá, Alcalá de Henares, Spain

11 #Current address: Product and Research Complex, Pasteur Institute of Iran, Karaj, Iran

12 **Running title:** mROS and cytokine-induced IFN- $\gamma$  in memory-like CD4<sup>+</sup> T cells

13 **Key words:** mitochondrial reactive oxygen species, IFN- $\gamma$ , IL-12/IL-18, Fas,  
14 effector/memory CD4 T cells

15 **\*Corresponding authors:**

16 Dr. Dimitrios Balomenos, Department of Immunology and Oncology, Centro Nacional  
17 de Biotecnología-Consejo Superior de Investigaciones Científicas (CNB-CSIC), Calle  
18 Darwin 3, Campus de Cantoblanco, 28049 Madrid, Spain. E-mail address:  
19 [dbalomenos@cnb.csic.es](mailto:dbalomenos@cnb.csic.es)

20 Dr. Gorjana Rackov, Department of Immunology and Oncology, Centro Nacional de  
21 Biotecnología-Consejo Superior de Investigaciones Científicas (CNB-CSIC), Calle

22 Darwin 3, Campus de Cantoblanco, 28049 Madrid, Spain. E-mail address:

23 [grackov@cnb.csic.es](mailto:grackov@cnb.csic.es)

24 **Abstract**

25 Mitochondrial activation and mROS production are crucial for CD4<sup>+</sup> T cell responses  
26 and have a role in naïve cell signaling after TCR activation. However, little is known  
27 about their role in recall responses driven by cytokine signaling. Here, we found that  
28 mROS are required for IL-12 plus IL-18-driven production of IFN- $\gamma$ , an essential  
29 cytokine in inflammatory and autoimmune disease development. In particular, memory-  
30 like cells obtained after activation-induced differentiation showed faster and augmented  
31 mROS accumulation and increased IFN- $\gamma$  production in response to IL-12 plus IL-18  
32 compared to naïve T cells. In contrast, mROS induction was similar in naïve and  
33 memory-like cells after TCR-dependent signaling. Taken together these results  
34 suggested that memory-like CD4<sup>+</sup> T cells treated by IL-12 plus IL-18 attained  
35 conditions for an extraordinary mROS-producing potential. mROS inhibition  
36 significantly downregulated the production of IFN- $\gamma$  and the expression of CD44  
37 activation marker, suggesting a direct mROS effect on the activation of memory-like T  
38 cells. Mechanistically, mROS was required for optimal activation of key signaling  
39 pathways that drive IFN- $\gamma$  production after IL-12 plus IL-18 T cell stimulation, such as  
40 PKC- $\theta$ , AKT and STAT4 phosphorylation, and NF- $\kappa$ B activation. Notably, we  
41 identified increased mROS as key promoters of hyperactivation and IFN- $\gamma$   
42 overproduction in Fas-deficient *lpr* memory-like CD4<sup>+</sup> T cells compared to WT cells,  
43 following IL-12 plus IL-18 stimulation. mROS inhibition significantly reduced the  
44 population of disease-associated CD44<sup>hi</sup>CD62L<sup>lo</sup> *lpr* CD4<sup>+</sup> T cells and their IFN- $\gamma$   
45 production. These findings uncover a previously unidentified role for Fas in regulating  
46 mitochondrial ROS production by memory-like T cells. This apoptosis-independent Fas  
47 activity might contribute to the accumulation of CD44<sup>hi</sup>CD62L<sup>lo</sup> CD4<sup>+</sup> T cells that  
48 produce increased IFN- $\gamma$  levels in *lpr* mice. Overall, our findings pinpoint mROS as

49 central regulators of TCR-independent signaling, and support mROS pharmacological

50 targeting to control aberrant immune responses in autoimmune-like disease.

51

## 52 **Introduction**

53 Upon TCR activation, mitochondria rapidly translocate to the immunological synapse,  
54 leading to electron transport chain (ETC) activation (1) and mitochondrial reactive  
55 oxygen species (mROS) production. Superoxide ( $O_2^{\cdot-}$ ) is generated at mitochondrial  
56 complexes I and III (2, 3), from where it can reach cytosol either directly through  
57 mitochondrial membrane or after conversion to hydrogen peroxide ( $H_2O_2$ ) (4). It has  
58 been established more recently that mROS play crucial role as redox signaling  
59 molecules in T cells, regulating IL-2 and IL-4 production upon TCR triggering (5, 6).

60 IL-12 and IL-18 are required to boost  $T_H1$  responses and IFN- $\gamma$  production after TCR  
61 ligation (7, 8). In a mechanism evolved to provide an early source of IFN- $\gamma$  and  
62 contribute to the innate immune response, IFN- $\gamma$  can be induced in a TCR-independent  
63 manner, only by IL-12 and IL-18 (9, 10). It has been proposed that this “cytokine-  
64 induced cytokine production” promotes chronic inflammation and autoimmunity (11,  
65 12). Indeed, we previously demonstrated that IFN- $\gamma$  production by *lpr* T cells creates a  
66 loop by increasing the macrophage inflammatory potential (13). The signaling  
67 mechanisms that drive IFN- $\gamma$  production in response to IL-12 plus IL-18 are distinct  
68 compared to those downstream of TCR, and lead to differential NF- $\kappa$ B recruitment to  
69 *Ifng* locus (14–16).

70 Although the role of mROS has been greatly appreciated downstream of TCR, their role  
71 in recall responses of previously activated  $CD4^+$  T cells and in IL-12 plus IL-18-  
72 dependent signaling regulation remains unexplored. Excessive production of ROS is  
73 thought to underlie some of the pathological immune reactions implicated in  
74 autoimmunity. T cells from lupus patients exhibit mitochondrial hyperpolarization,  
75 resulting in increased mROS production (17, 18). In a previous study, we demonstrated

76 that autoimmune traits in *lpr* mice were decreased by controlling autoreactive T cell  
77 hyperactivation and their IFN- $\gamma$  overproduction (13). However, the direct link between  
78 mROS and IFN- $\gamma$  hyperproduction in autoreactive T cells has not been made thus far.

79 Here, we hypothesized that mROS act as driving force to modulate signal transduction  
80 leading to hyperproduction of IFN- $\gamma$ . We analyzed the role of mROS in IL-12 plus IL-  
81 18-induced IFN- $\gamma$  production in naïve and in *in vitro*-differentiated memory-like CD4<sup>+</sup>  
82 T cells, and found significantly higher amounts of mROS and IFN- $\gamma$  in the later. We  
83 demonstrated that mROS signal controls STAT4 and NF- $\kappa$ B activation pathways.  
84 Finally, we showed that Fas-deficient CD4<sup>+</sup> T cells produce more mROS compared to  
85 WT in response to IL-12 plus IL-18. This was translated to greatly increased IFN- $\gamma$   
86 production and to higher proportions of CD44<sup>hi</sup>CD62L<sup>lo</sup> *lpr* CD4<sup>+</sup> T cells compared to  
87 WT. Our findings establish mROS as key component of TCR-independent IFN- $\gamma$   
88 production and uncover an unknown role of Fas in regulating mROS and IFN- $\gamma$   
89 production, providing rationale for targeting mROS in autoimmunity-related  
90 hyperinflammation.

## 91 **Materials and Methods**

### 92 **Animals**

93 8-12 weeks old mice were used for CD4<sup>+</sup> T cell isolation. C57BL/6 mice (WT) were  
94 from Harlan Interfauna Ibérica and Fas-deficient C57BL/6-*lpr* mice (*lpr*) were from  
95 Jackson laboratories. Mice were kept in SPF conditions. All animal experiments were  
96 designed in compliance with European Union and national regulations, and were  
97 approved by the CNB Bioethics Committee.

### 98 ***In vitro* CD4<sup>+</sup> T cell activation and memory-like differentiation**

99 Naïve CD4<sup>+</sup> T cells were purified from mouse spleens using Negative Isolation Kit  
100 (DynaL Biotech). Cell purity was >95% as measured by flow cytometry. For cell culture,  
101 we used complete media containing 20 ng/ml human recombinant interleukin-2 (rIL-2,  
102 PeproTech). Naïve CD4<sup>+</sup> T cells (10<sup>6</sup>/ml) were stimulated with concavalin A (ConA;  
103 1.5 µg/ml, Sigma) or with IL-12 (10 ng/ml) plus IL-18 (10 ng/ml) for indicated time  
104 points. For memory-like differentiation, naïve CD4<sup>+</sup> T cells were first stimulated with  
105 ConA (1.5 µg/ml) for 24h, washed and cultured (0.5 x 10<sup>6</sup>/ml) in presence of 20 ng/ml  
106 rIL-2 for 6 days. Differentiated memory-like cells were stimulated with ConA or with  
107 IL-12 (10 ng/ml) plus IL-18 (10 ng/ml) for indicated time points. DPI (5 µM; Sigma),  
108 rotenone (2.5 µM; Sigma) or antimycin A (4 µM) were added to cell culture 30 min  
109 before the stimulus.

### 110 **Flow cytometry**

111 For detection of mitochondrial superoxide, cells were incubated with MitoSOX Red  
112 (Invitrogen) at 5 µM final concentration for 30 min at 37 °C and stimulated for

113 indicated time points. Cells were then washed with PBS, centrifuged at  $300 \times g$  for 5  
114 min, and analyzed immediately using flow cytometry. MitoSOX Red fluorescence was  
115 detected at the excitation and emission wavelengths of 488 and 585 nm, respectively.  
116 To control for baseline fluorescence, samples from each experiment were stained  
117 according to the above procedure and left unstimulated. MFI fold induction was  
118 calculated by dividing stimulated by unstimulated values.

119 For measurement of mitochondrial membrane potential TMRM  
120 (Tetramethylrhodamine, Methyl Ester, Perchlorate; ThermoFisher) was added to the  
121 cells at 30 nM final concentration. After 30 min, cells were analyzed by flow cytometry.  
122 Control cells were pre-incubated with 5  $\mu$ M FCCP for 10 min at 37 °C to depolarize the  
123 membrane and show background staining.

124 Intracellular cytokine staining and cell cycle analysis were performed according to  
125 standard procedure described in Supplementary Material. Stained cells were analyzed  
126 on Gallios flow cytometer from Beckman Coulter. The data were analyzed using  
127 FlowJo software (Tree Star).

## 128 **Immunoblotting**

129 Cells were treated as stated and the immunoblotting was performed as described in  
130 Supplementary Material.

## 131 **EMSA**

132 EMSA was performed as described previously (19) and described in Supplementary  
133 Material.

## 134 **Statistical Analysis**



135 Statistical significance was determined by unpaired 2-tailed Student's *t* test for  
136 comparisons between two groups, or by 1- or 2-way ANOVA for multiple comparisons,  
137 followed by Sidak's or Tukey post-hoc test. Differences were considered significant  
138 when  $p < 0.05$ . All statistical analyses were conducted using Prism 8 software  
139 (GraphPad).

140 **Results**

141 **Memory-like CD4<sup>+</sup> T cells produce increased mROS and IFN- $\gamma$  in response to IL-**  
142 **12/IL-18 compared with naïve cells**

143 Naïve CD4<sup>+</sup> T cells purified from mouse spleens were stimulated *ex vivo* with IL-12/IL-  
144 18 to induce IFN- $\gamma$  production independently of TCR, as previously described (20).  
145 Alternatively, T cells were exposed to concavalin A (ConA), which is known for  
146 mimicking the physiological TCR cross-linking leading to T cell activation and ROS  
147 production (21). After primary TCR activation and IL-2 dependent culture, memory-  
148 like CD4<sup>+</sup> T cells were re-stimulated with either ConA or with IL-12/IL-18. As  
149 previously described (22), naïve CD4<sup>+</sup> T cells, characterized by CD62L<sup>hi</sup>CD44<sup>lo</sup>  
150 phenotype, efficiently differentiated into central and effector memory cell subsets after  
151 IL-2 expansion (Supplementary Figure 1). Upon 24 h of TCR stimulation, intracellular  
152 staining showed significant but relatively low IFN- $\gamma$  production both after primary and  
153 secondary activation of naïve and memory-like cells, respectively (Figure 1A).  
154 IL-12/IL-18 stimulation induced similar IFN- $\gamma$  levels as ConA in naïve CD4<sup>+</sup> cells  
155 (Figure 1A). By contrast, the proportions of IFN- $\gamma$ -producing cells after IL-12/IL-18  
156 stimulation were strikingly higher in memory-like compared with naïve cells (Figure  
157 1A). The data showed that IL-12/IL-18 induce IFN- $\gamma$  more efficiently in memory-like  
158 CD4<sup>+</sup> T cells compared to TCR-dependent stimulation.

159 We measured mitochondrial superoxide production with MitoSOX Red in naïve and  
160 memory-like T cells after TCR-dependent and -independent stimulation. After ConA  
161 treatment, the percentage of MitoSOX<sup>hi</sup> cells was significantly increased compared to  
162 unstimulated cells, but we found no significant differences in mROS production  
163 between naïve and memory-like cells (Figure 1B). In naïve cells, the proportions of

164 MitoSox<sup>hi</sup> cells after IL-12/IL-18 stimulation were similar to those induced by ConA  
165 (Figure 1B). However, IL-12/IL-18 induced significantly higher proportions of  
166 MitoSOX<sup>hi</sup> cells in the memory-like cell population compared to that of naïve cells  
167 (Figure 1B). We also measured MitoSOX MFI and obtained similar results  
168 (Supplementary Figure 2).

169 These data showed that memory-like cells displayed enhanced responses after IL-12/IL-  
170 18 compared to ConA stimulation in terms of both IFN- $\gamma$  and mROS production, while  
171 the two types of stimulation had similar effects on naïve T cells.

### 172 **IL-12/IL-18-dependent IFN- $\gamma$ production by naïve CD4<sup>+</sup> T cells requires mROS** 173 **activation**

174 To investigate whether mROS are functionally related to IL-12/IL-18-induced  
175 IFN- $\gamma$  production by naïve CD4<sup>+</sup> T cells, we inhibited mROS production using DPI  
176 (diphenyleneiodonium) (23, 24). Alternatively, we used specific mitochondrial complex  
177 I inhibitor rotenone.

178 Upon T cell stimulation we detected two cell populations: MitoSOX<sup>lo</sup> and MitoSOX<sup>hi</sup>  
179 cells. While in MitoSOX<sup>hi</sup> cell population MitoSOX MFI significantly increased at 30-  
180 and 60-min post IL-12/IL-18 or ConA stimulation, MitoSOX<sup>lo</sup> cells remained  
181 unresponsive (Supplementary Figure 3 and data not shown). We therefore focused our  
182 analyses on the MitoSOX<sup>hi</sup> population, which represented activated T cells.

183 We analyzed early MitoSOX levels with or without mROS inhibitors after T cell  
184 activation over a period of two hours. MitoSOX was significantly increased at 30 min  
185 post stimulation and remained elevated for at least two hours, as indicated by MitoSOX  
186 median fluorescence intensity (MFI) (Figure 2A). At all time points up to 2 h post-

187 stimulation, the activation-induced mROS increase was dramatically suppressed upon  
188 DPI treatment, to mROS levels of unstimulated cells (Figure 2A). These data show that  
189 DPI inhibits mROS production in cells that are responsive to IL-12/IL-18. Similar  
190 results were obtained using rotenone (not shown).

191 IL-12/IL-18 stimulation of naïve T cells induced IFN- $\gamma$  production in a low cell  
192 proportion (~1.5%) that were also CD44<sup>hi</sup>, at 24h post-stimulation (Figure 2B, left).  
193 Importantly, DPI treatment reduced IFN- $\gamma$  production by these cells (Figure 2B, left) in  
194 a statistically significant manner (Figure 2B, right). However, DPI had no effect on the  
195 expression of CD44 (Figure 2C). Overall, our results suggest that mROS control IFN- $\gamma$   
196 production after activation of naïve CD4<sup>+</sup> T cells.

197 **mROS inhibition lowers IFN- $\gamma$  production by memory-like CD4<sup>+</sup> T cells and**  
198 **compromises their CD44<sup>hi</sup> phenotype**

199 Memory-like CD4<sup>+</sup> T cells generated after primary TCR activation and IL-2-dependent  
200 culture significantly increased mROS production as early as 15 min post IL-12/IL-18  
201 stimulation (Figure 3A). The impact of mROS on cytokine-induced signaling is likely  
202 more relevant in memory-like than in naïve CD4<sup>+</sup> T cells, as in the later mROS increase  
203 was not detected until 30 min post-stimulation (Figure 2A).

204 DPI led to a prominent reduction of mROS, as detected by MitoSOX at all time points  
205 tested after IL-12/IL-18 treatment (Figure 3A). Memory-like cells were more responsive  
206 to IL-12/IL-18 stimulation compared to naïve cells, as ~10% of the total CD4<sup>+</sup>  
207 population were CD44<sup>hi</sup> cells and positive for IFN- $\gamma$  at 24 h post-stimulation (Figure  
208 3B). The mROS inhibitor DPI nearly abrogated IFN- $\gamma$  production in memory-like T  
209 cells (Figure 3B, left) in statistically significant manner (Figure 3B, right). In addition,

210 DPI led to significant downregulation of CD44 expression, suggesting that mROS  
211 regulates the activation potential of memory-like T cells (Figure 3C). Of note, we didn't  
212 observe any marked effect of DPI treatment on cell viability nor on cell cycle  
213 distribution (Supplementary Figure 4A). Our results support the notion that mROS are  
214 integral to the maintenance of activated CD44<sup>hi</sup> phenotype and control the TCR-  
215 independent IFN- $\gamma$  production.

### 216 **Validation of DPI as an attenuator of IFN- $\gamma$ production through inhibition of** 217 **mROS production**

218 Our results showed that DPI strongly inhibits mROS-dependent IFN- $\gamma$  production by  
219 memory-like CD4<sup>+</sup> T cells. DPI is also known for inhibiting Nox enzymes (23, 25–27),  
220 raising questions of whether the observed effects of DPI on IFN- $\gamma$  production might be  
221 due to mitochondria-unrelated processes. To address this point and validate the effect of  
222 mROS generation on IFN- $\gamma$  production we tested other respiratory chain blockers.  
223 Specific complex I inhibitor rotenone significantly decreased IL-12/IL-18-induced  
224 mROS production (Figure 4A), as well as the percentages of IFN- $\gamma$ -producing and  
225 CD44<sup>hi</sup> cells (Figure 4B), thus providing similar results as DPI. We also used antimycin  
226 A, an electron transport chain inhibitor acting at complex III. Although antimycin A has  
227 been shown to increase mROS production (28), we found that in the present setting it  
228 does not affect mROS at early time points post-IL-12/IL-18 stimulation (Figure 4A). In  
229 addition, antimycin A was not effective in blocking IFN- $\gamma$  production nor in reducing  
230 CD44 expression, suggesting that an intact electron transport chain is not required for  
231 IL-12/IL-18-induced IFN- $\gamma$  production.

232 Other studies have shown that DPI treatment might affect the overall electron transport  
233 activity and mitochondrial membrane potential (29). We therefore used potentiometric

234 TMRM dye to test whether DPI treatment affects the mitochondrial membrane potential  
235 during memory-like CD4<sup>+</sup> T cell activation. TMRM fluorescence showed that neither  
236 IL-12/IL-18 nor DPI significantly affected mitochondrial membrane potential at early  
237 time points after stimulation (Figure 4C). Thus, it seems that mROS inhibition did not  
238 affect the overall electron transport rate, in accordance with previous studies (29).

### 239 **mROS-mediated signals activate PKC- $\theta$ , AKT, STAT4 and NF- $\kappa$ B**

240 IL-12 and IL-18 act in synergy through different signaling pathways to activate IFN- $\gamma$   
241 production (30). IL-12 receptor stimulation leads to STAT4 phosphorylation through  
242 Jak2 and Tyk2, while IL-18 (also known as IFN- $\gamma$ -inducing factor) activates the NF- $\kappa$ B  
243 pathway via IRAK (interleukin 1 receptor-associated kinase) and TRAF6 (TNF  
244 receptor-associated factor 6) (20, 31, 32). We examined the components of these two  
245 pathways in memory-like CD4<sup>+</sup> T cells before and after treatment with mROS inhibitors  
246 DPI or rotenone. Before IL-12/IL-18 treatment the NF- $\kappa$ B pathway was kept in its  
247 latent state, as seen by high protein levels of I $\kappa$ B $\alpha$  (Figure 5 A, Ctrl). Stimulation  
248 induced NF- $\kappa$ B activation, as I $\kappa$ B $\alpha$  levels dropped as early as 15 min and 30 min  
249 (highest reduction) post-stimulation (Figure 5A and B). After DPI or rotenone treatment  
250 this drop in I $\kappa$ B $\alpha$  was halted, suggesting that NF- $\kappa$ B activation is delayed in conditions  
251 of decreased mROS. We also examined the activation of PKC- $\theta$ , as it has been  
252 previously implicated in TCR-independent NF- $\kappa$ B regulation (33). We found increased  
253 PKC- $\theta$  phosphorylation as early as 15 min post-IL-12/IL-18 treatment (Figure 5A and  
254 B). Both inhibitors reduced the phospho-PKC- $\theta$  levels, which was evident at 30 min  
255 and more so at 1 h post-treatment. These data suggest that early mitochondrial oxidative  
256 signal promotes PKC- $\theta$  and NF- $\kappa$ B activation after IL-12/IL-18 signaling. In  
257 accordance with this, electromobility shift showed elevated NF- $\kappa$ B nuclear activity at

258 1h post-IL-12/IL-18 treatment, which was markedly decreased by DPI or rotenone  
259 (Figure 5C).

260 STAT4 is key transcription factor recruited by IL-12-derived signal to regulate IFN- $\gamma$   
261 (31). Phosphorylation of STAT4 was evident after IL-12 plus IL-18 stimulation (Figure  
262 5D). Both after rotenone and DPI treatment, STAT4 phosphorylation was markedly  
263 decreased early after IL-12/IL-18 stimulation (Figure 5D). This suggested a direct  
264 mROS role in IL-12-dependent STAT4 activation. IL-18 in certain cell types activates  
265 AKT (34), and mROS affects AKT phosphorylation (35). We detected increased AKT  
266 phosphorylation after IL-12/IL-18 treatment (Figure 5D). mROS inhibition using  
267 rotenone or DPI markedly decreased phospho-AKT levels (Figure 5D).

268 Altogether, these data further strengthen the notion that mROS trigger the early  
269 signaling events downstream of IL-12 and IL-18 receptors leading to IFN- $\gamma$  production  
270 independently of TCR activation.

271 **IFN- $\gamma$  hyperproduction in *lpr* CD44<sup>hi</sup>CD62L<sup>lo</sup> effector/memory CD4<sup>+</sup> T cells is**  
272 **related to increased mROS**

273 *lpr* (lymphoproliferation spontaneous mutation) mice are Fas (CD95) deficient and  
274 show defective AICD (activation-induced cell death) of *in vitro* re-stimulated T cells  
275 (36, 37). *In vivo*, one of the symptoms caused by Fas deficiency in *lpr* mice is the  
276 accumulation of effector/memory CD44<sup>hi</sup>CD62L<sup>lo</sup> CD4<sup>+</sup> T cells and their intrinsic  
277 hyperactivation accompanied by hyperproduction of IFN- $\gamma$  in response to IL-12/IL-  
278 18 (13). To investigate the role of mROS in the responses of Fas-deficient memory-like  
279 cells, we purified CD4<sup>+</sup> T cells from WT and *lpr* mice and, after initial ConA  
280 stimulation and IL-2 expansion, we stimulated the cells with IL-12/IL-18. Significantly

281 higher mROS levels were induced in *lpr* compared with WT cells, as seen by MitoSOX  
282 at 60 min after stimulation (Figure 6A). The mROS production was greatly diminished  
283 by DPI in both WT and *lpr* cells (Figure 6B). Of note, the proportions of CD44<sup>hi</sup> cells  
284 were similar between WT and *lpr*, suggesting that Fas deficiency did not cause  
285 increased accumulation of memory-like cells under these experimental conditions and  
286 TCR-independent stimulation (Figure 6C). Accordingly, cell cycle analysis showed no  
287 apparent difference in apoptosis or proliferation in WT and *lpr* CD4<sup>+</sup> T cells after IL-12  
288 plus IL-18 stimulation (Supplementary Figure 4B). Instead, *lpr* CD44<sup>hi</sup> T cells were  
289 hyperactivated, as seen by significantly increased IFN- $\gamma$  production compared to WT  
290 cells (~20 vs. 30% of the total CD4<sup>+</sup> population) at 24 h post-IL-12/IL-18 (Figure 6D).  
291 DPI treatment significantly reduced the IFN- $\gamma$  production in both WT and *lpr* CD44<sup>hi</sup> T  
292 cells (Figure 6D). These results suggest that the increased mROS production drives the  
293 increased IFN- $\gamma$  production by *lpr* CD44<sup>hi</sup> T cells.

294 *lpr* CD4<sup>+</sup> T cells showed increased proportions of CD44<sup>hi</sup>/CD62L<sup>lo</sup> effector/memory  
295 cells compared with the WT (~30 vs. 50%), which were further increased after IL-  
296 12/IL-18 treatment (~58 vs. 73%, Figure 6E). Although DPI did not affect CD62L<sup>hi</sup> and  
297 CD62L<sup>lo</sup> proportions in WT cells, it significantly reduced the population of *lpr*  
298 CD44<sup>hi</sup>/CD62L<sup>lo</sup> effector/memory cells, to the levels comparable to those in the WT cell  
299 population (Figure 6E). Altogether, our results corroborate that the increased mROS  
300 production drives not only the hyperactivation and increased potential for IFN- $\gamma$   
301 production in Fas-deficient CD4<sup>+</sup> T cells, but also their intensified differentiation  
302 towards the effector/memory CD44<sup>hi</sup>/CD62L<sup>lo</sup> phenotype. This points to Fas as a  
303 regulator of mitochondrial ROS that ultimately controls the status of memory-like T  
304 cells independently of the proapoptotic role of Fas in such cells.



## 305 **Discussion**

306 It is established that TCR engagement induces mitochondrial activation and mROS  
307 production that modulates the redox state of signaling molecules governing the early  
308 events downstream of TCR induction. Here, we analyzed the role of mROS in recall  
309 responses of memory-like T cells. mROS induction was similar in naïve and memory-  
310 like cells after TCR-dependent signaling, while in response to IL-12 plus IL-18  
311 memory-like CD4<sup>+</sup> T cells showed a great and highly significant increase in mROS and  
312 IFN- $\gamma$  production compared to naïve T cells. This suggested that memory-like CD4<sup>+</sup> T  
313 cells stimulated by IL-12 plus IL-18 acquired a singular capacity in producing mROS,  
314 and our study was geared at examining the effect of such TCR-independent triggering.  
315 We report the following major findings: 1) Inhibition of the increased mROS  
316 production by memory-like T cells after exposure to IL-12 plus IL-18 was directly  
317 associated to IFN- $\gamma$  production and to maintaining the memory-like phenotype of  
318 stimulated cells; 2) The mechanism that drives IFN- $\gamma$  production is regulated by the  
319 effect of mROS on the activation of the pathways that depend on IL-12 plus IL-18  
320 signaling; 3) Our results uncovered a previously unknown Fas role as a regulator of  
321 mROS induction, since *lpr* memory-like CD4<sup>+</sup> T cells produced higher mROS levels  
322 compared to WT cells, leading to elevated IFN- $\gamma$  and increased differentiation to  
323 effector/ memory T cells.

324 TCR stimulation of CD4<sup>+</sup> cells triggers the early production of mROS, which act as  
325 secondary messengers in regulating IL-2 production and cell proliferation (6, 38).  
326 Additionally, at later stages of CD4<sup>+</sup> T cells stimulation, mitochondrial activity and  
327 mROS production are increased (39). Mitochondria activation is associated with  
328 enhanced recall responses of memory CD8<sup>+</sup> T cells after TCR-dependent restimulation,

329 but a possible mROS association with memory T cell responses was not assessed (40).  
330 Nevertheless, cytosolic ROS was found increased in *in vitro* memory-like CD4<sup>+</sup> T cells  
331 after TCR dependent stimulation (5). In our study we found similar mROS levels in  
332 naïve and memory-like CD4<sup>+</sup> T cells early after TCR activation. We used IL-12 plus IL-  
333 18 stimulation to investigate the role of mROS in memory-like CD4<sup>+</sup> T cells, a protocol  
334 that did not induce T cell apoptosis or proliferation, but greatly increased mROS in  
335 memory-like compared to naïve T cells after activation. Overall, our findings suggest  
336 that mROS production in T cells depends on their activation state and the stimulus type.

337 mROS levels were directly linked to the hyperactivation status of T cells in response to  
338 IL-12 plus IL-18 induction, as inhibition of mROS production by DPI or Rotenone  
339 reflected a greatly lowered IFN- $\gamma$  expression and the diminished expression of the CD44  
340 activation/memory marker. Apart from mROS, other aspects of mitochondrial activity  
341 are needed for correct T cell function and TCR-induced activation. As part of the  
342 immunological synapse, mitochondria participate in Ca<sup>2+</sup> uptake and thus determine  
343 amplitude and duration of Ca<sup>2+</sup> signal. Mitochondrial uncoupling results in inhibition of  
344 the TCR-induced Ca<sup>2+</sup> signal due to diminished mitochondrial membrane potential and  
345 reduced ability to prolong Ca influx (41). In our approach the mitochondrial membrane  
346 potential remained unaffected by mROS inhibition, indicating that mROS is the  
347 promotor of memory-T cell hyperactivation.

348 IFN- $\gamma$  production is induced through synergy of signaling driven by IL-12R and IL-18R  
349 stimulation pathways (30). mROS inhibition reduced IL-12R-dependent STAT4  
350 phosphorylation and IL-18-dependent NF- $\kappa$ B activation, indicating that mROS drive  
351 signaling of both pathways. Kinetic analysis showed that mROS affects these pathways  
352 early on after exposure of cells to IL-12 plus IL-18. Other molecules such as PKC- $\theta$  or

353 AKT linked to these pathways showed increased phosphorylation due to increased  
354 mROS. The redox conditions that are associated to increased mROS production, could  
355 be responsible for alteration in phosphorylation patterns, as kinase and phosphatase  
356 activities are redox-dependent. Whether the increased mROS activate specific pathway  
357 components or have a multiple effect in the phosphorylation and activation remains to  
358 be explored. Another important issue is to understand the reasons behind the specificity  
359 of mROS production after secondary IL-12 plus IL-18 stimulation. We hypothesize that  
360 components of the IL-12R or the IL-18R signaling pathways may drive ETC  
361 respiration. Indeed, PKC- $\theta$  (28) is shown to interact with and activate mitochondria, and  
362 Tyk2 that forms part of the Jak family and a component of the IL-12R signaling  
363 regulates mitochondrial activation (42).

364 Compared to normal T cells, *lpr* memory-like CD4<sup>+</sup> overproduced mROS and IFN- $\gamma$   
365 after IL-12 plus IL-18 activation. Inhibition of mROS induction reduced not only the  
366 elevated IFN- $\gamma$  but also the CD44<sup>hi</sup>/CD62L<sup>lo</sup> effector/memory cells that are responsible  
367 for the *in vivo* IFN- $\gamma$  and lupus-like symptoms of *lpr* mice (13). Thus, our data suggest  
368 that Fas through non-apoptotic signaling (IL-12/IL-18) limits the production of mROS,,  
369 compromising differentiation into effector/memory T cells and IFN- $\gamma$  overproduction.  
370 This might provide a feedback mechanism to control T cell homeostasis under chronic  
371 inflammation and prevent development of autoimmunity. Therefore, uncontrolled  
372 mROS production by T cells in *lpr* mice or humans with ALPS (autoimmune lympho-  
373 proliferative syndrome) (43) might favor lymphadenopathy development, as mROS  
374 inhibition lowers Fas-dependent AICD (28). Other non-apoptotic Fas roles have been  
375 described, especially after primary T cell stimulation (44). Further studies are clearly  
376 needed for the better understanding of the mechanism that would explain the effect of  
377 Fas on mROS regulation. Overall, the results unveil a previously unknown apoptosis-

378 independent role of Fas in regulating mROS production and associated  
379 hyperinflammatory outcomes. Our findings identify mROS as a driver of inflammation  
380 in *lpr* disease and potentially other autoimmune disorders. These observations strongly  
381 suggest that blockade of mROS provides a therapeutic strategy to decrease  
382 inflammation in T cell-mediated inflammatory disorders.

383 **Acknowledgements**

384 This work was funded by the grant from Comunidad de Madrid (CAM; B2017/BMD-  
385 3804) to D. Balomenos. G. Rackov holds postdoctoral Juan de la Cierva Fellowship.  
386 None of the funding institutions had the role in the design of the study and collection,  
387 analysis and interpretation of the data and writing of the manuscript.

388 **Conflict of interest**

389 The authors declare no competing financial interest in relation to the work described.

390 **Availability of data and materials**

391 All data generated and analyzed during this study are included in this article.

392 **Authors' contributions**

393 DB and GR conceived and designed the study, analyzed the data and wrote the  
394 manuscript. CMA and MAM provided input in designing the project. GR, PTZ, SCP  
395 and RS performed the experiments. All authors read, discussed and approved the  
396 manuscript.

397 **References**

- 398 1. Tarasov, A. I., E. J. Griffiths, and G. A. Rutter. 2012. Regulation of ATP production  
399 by mitochondrial Ca(2+). *Cell Calcium* 52: 28–35.
- 400 2. Koopman, W. J. H., L. G. J. Nijtmans, C. E. J. Dieteren, P. Roestenberg, F.  
401 Valsecchi, J. A. M. Smeitink, and P. H. G. M. Willems. 2010. Mammalian  
402 mitochondrial complex I: biogenesis, regulation, and reactive oxygen species  
403 generation. *Antioxid. Redox Signal.* 12: 1431–70.
- 404 3. Desdín-Micó, G., G. Soto-Herederó, and M. Mittelbrunn. 2018. Mitochondrial  
405 activity in T cells. *Mitochondrion* 41: 51–57.
- 406 4. Han, D., F. Antunes, R. Canali, D. Rettori, and E. Cadenas. 2003. Voltage-dependent  
407 anion channels control the release of the superoxide anion from mitochondria to cytosol.  
408 *J. Biol. Chem.* 278: 5557–63.
- 409 5. Kaminski, M. M., S. W. Sauer, C.-D. Klemke, D. Süß, J. G. Okun, P. H. Krammer,  
410 and K. Gülow. 2010. Mitochondrial reactive oxygen species control T cell activation by  
411 regulating IL-2 and IL-4 expression: mechanism of ciprofloxacin-mediated  
412 immunosuppression. *J. Immunol.* 184: 4827–4841.
- 413 6. Sena, L. A., S. Li, A. Jairaman, M. Prakriya, T. Ezponda, D. A. Hildeman, C. R.  
414 Wang, P. T. Schumacker, J. D. Licht, H. Perlman, P. J. Bryce, and N. S. Chandel. 2013.  
415 Mitochondria Are Required for Antigen-Specific T Cell Activation through Reactive  
416 Oxygen Species Signaling. *Immunity* 38: 225–236.
- 417 7. Trinchieri, G. 1994. Interleukin-12: a cytokine produced by antigen-presenting cells  
418 with immunoregulatory functions in the generation of T-helper cells type 1 and  
419 cytotoxic lymphocytes. *Blood* 84: 4008–27.
- 420 8. Okamura, H., S. Kashiwamura, H. Tsutsui, T. Yoshimoto, and K. Nakanishi. 1998.  
421 Regulation of interferon- $\gamma$  production by IL-12 and IL-18. *Curr Opin Immunol* 10: 259–

- 422 264.
- 423 9. Yang, J., H. Zhu, T. L. Murphy, W. Ouyang, and K. M. Murphy. 2001. IL-18-  
424 stimulated GADD45 $\beta$  required in cytokine-induced, but not TCR-induced, IFN- $\gamma$   
425 production. *Nat. Immunol.* 2: 157–164.
- 426 10. Munk, R. B., K. Sugiyama, P. Ghosh, C. Y. Sasaki, L. Rezanka, K. Banerjee, H.  
427 Takahashi, R. Sen, and D. L. Longo. 2011. Antigen-independent IFN- $\gamma$  production by  
428 human naïve CD4<sup>+</sup> T cells activated by IL-12 plus IL-18. *PLoS One* 6: 1–8.
- 429 11. Yu, J. J., C. S. Tripp, and J. H. Russell. 2003. Regulation and Phenotype of an  
430 Innate Th1 Cell: Role of Cytokines and the p38 Kinase Pathway. *J. Immunol.* 171:  
431 6112–6118.
- 432 12. Sattler, A., U. Wagner, M. Rossol, J. Sieper, P. Wu, A. Krause, W. A. Schmidt, S.  
433 Radmer, S. Kohler, C. Romagnani, and A. Thiel. 2009. Cytokine-induced human IFN- $\gamma$ -  
434 secreting effector-memory Th cells in chronic autoimmune inflammation. *Blood* 113:  
435 1948–1956.
- 436 13. Daszkiewicz, L., C. Vázquez-Mateo, G. Rackov, A. Ballesteros-Tato, K. Weber, A.  
437 Madrigal-Avilés, M. Di Pilato, A. Fotedar, R. Fotedar, J. M. Flores, M. Esteban, C.  
438 Martínez-A, and D. Balomenos. 2015. Distinct p21 requirements for regulating normal  
439 and self-reactive T cells through IFN- $\gamma$  production. *Sci. Rep.* 5: 7691.
- 440 14. Papadakis, K. A., D. Zhu, J. L. Prehn, C. Landers, A. Avanesyan, G. Lafkas, and S.  
441 R. Targan. 2005. Dominant Role for TL1A/DR3 Pathway in IL-12 plus IL-18-Induced  
442 IFN- $\gamma$  Production by Peripheral Blood and Mucosal CCR9<sup>+</sup> T Lymphocytes. *J.*  
443 *Immunol.* 174: 4985–4990.
- 444 15. Balasubramani, A., Y. Shibata, G. E. Crawford, A. S. Baldwin, R. D. Hatton, and C.  
445 T. Weaver. 2010. Modular utilization of distal cis-regulatory elements controls Ifng  
446 gene expression in T cells activated by distinct stimuli. *Immunity* 33: 35–47.

- 447 16. Yang, J., T. L. Murphy, W. Ouyang, and K. M. Murphy. 1999. Induction of  
448 interferon- $\gamma$  production in Th1 CD4+ T cells: Evidence for two distinct pathways for  
449 promoter activation. *Eur. J. Immunol.* 29: 548–555.
- 450 17. Gergely, P., B. Niland, N. Gonchoroff, R. Pullmann, P. E. Phillips, and A. Perl.  
451 2002. Persistent mitochondrial hyperpolarization, increased reactive oxygen  
452 intermediate production, and cytoplasmic alkalinization characterize altered IL-10  
453 signaling in patients with systemic lupus erythematosus. *J. Immunol.* 169: 1092–101.
- 454 18. Perl, A. 2013. Oxidative stress in the pathology and treatment of systemic lupus  
455 erythematosus. *Nat. Rev. Rheumatol.* 9: 674–686.
- 456 19. Rackov, G., E. Hernández-Jiménez, R. Shokri, L. Carmona-Rodríguez, S. Mañes,  
457 M. Álvarez-Mon, E. López-Collazo, C. Martínez-A, and D. Balomenos. 2016. p21  
458 mediates macrophage reprogramming through regulation of p50-p50 NF- $\kappa$ B and IFN-  
459  $\beta$ . *J. Clin. Invest.* 126: 3089–103.
- 460 20. Robinson, D., K. Shibuya, A. Mui, F. Zonin, E. Murphy, T. Sana, S. B. Hartley, S.  
461 Menon, R. Kastelein, F. Bazan, and A. O. Garra. 1997. IGIF Does Not Drive Th1  
462 Development but Synergizes with IL-12 for Interferon-g Production and Activates  
463 IRAK and NF $\kappa$ B. *Immunity* 7: 571–581.
- 464 21. Pani, G., R. Colavitti, S. Borrello, and T. Galeotti. 2000. Endogenous oxygen  
465 radicals modulate protein tyrosine phosphorylation and JNK-1 activation in lectin-  
466 stimulated thymocytes. *Biochem. J.* 347: 173–181.
- 467 22. Cruz, A. C., M. Ramaswamy, C. Ouyang, C. A. Klebanoff, P. Sengupta, T. N.  
468 Yamamoto, F. Meylan, S. K. Thomas, N. Richoz, R. Eil, S. Price, R. Casellas, V. K.  
469 Rao, J. Lippincott-Schwartz, N. P. Restifo, and R. M. Siegel. 2016. Fas/CD95 prevents  
470 autoimmunity independently of lipid raft localization and efficient apoptosis induction.  
471 *Nat. Commun.* 7.



- 472 23. Li, Y., and M. A. Trush. 1998. Diphenyleneiodonium, an NAD(P)H oxidase  
473 inhibitor, also potently inhibits mitochondrial reactive oxygen species production.  
474 *Biochem. Biophys. Res. Commun.* 253: 295–299.
- 475 24. Bulua, A. C., A. Simon, R. Maddipati, M. Pelletier, H. Park, K.-Y. Kim, M. N.  
476 Sack, D. L. Kastner, and R. M. Siegel. 2011. Mitochondrial reactive oxygen species  
477 promote production of proinflammatory cytokines and are elevated in TNFR1-  
478 associated periodic syndrome (TRAPS). *J. Exp. Med.* 208: 519–33.
- 479 25. Vendrov, A. E., N. R. Madamanchi, Z. S. Hakim, M. Rojas, and M. S. Runge. 2006.  
480 Thrombin and NAD(P)H oxidase-mediated regulation of CD44 and BMP4-Id pathway  
481 in VSMC, restenosis, and atherosclerosis. *Circ. Res.* 98: 1254–1263.
- 482 26. Cross, A. R., and O. T. Jones. 1986. The effect of the inhibitor diphenylene  
483 iodonium on the superoxide-generating system of neutrophils. Specific labelling of a  
484 component polypeptide of the oxidase. *Biochem. J.* 237: 111–116.
- 485 27. Devadas, S., L. Zaritskaya, S. G. Rhee, L. Oberley, and M. S. Williams. 2002.  
486 Discrete generation of superoxide and hydrogen peroxide by T cell receptor stimulation:  
487 selective regulation of mitogen-activated protein kinase activation and fas ligand  
488 expression. *J. Exp. Med.* 195: 59–70.
- 489 28. Kaminski, M., M. Kiessling, D. Süß, P. H. Krammer, and K. Gülow. 2007. Novel  
490 role for mitochondria: protein kinase C $\theta$ -dependent oxidative signaling organelles in  
491 activation-induced T-cell death. *Mol. Cell. Biol.* 27: 3625–3639.
- 492 29. Lambert, A. J., J. A. Buckingham, H. M. Boysen, and M. D. Brand. 2008.  
493 Diphenyleneiodonium acutely inhibits reactive oxygen species production by  
494 mitochondrial complex I during reverse, but not forward electron transport. *Biochim.*  
495 *Biophys. Acta - Bioenerg.* 1777: 397–403.
- 496 30. Nakahira, M., H.-J. Ahn, W.-R. Park, P. Gao, M. Tomura, C.-S. Park, T. Hamaoka,

- 497 T. Ohta, M. Kurimoto, and H. Fujiwara. 2002. Synergy of IL-12 and IL-18 for IFN-  
498 gamma gene expression: IL-12-induced STAT4 contributes to IFN-gamma promoter  
499 activation by up-regulating the binding activity of IL-18-induced activator protein 1. *J.*  
500 *Immunol.* 168: 1146–1153.
- 501 31. Bacon, C. M., E. F. Petricoin, J. R. Ortaldo, R. C. Rees, A. C. Larner, J. A.  
502 Johnston, and J. J. O’Shea. 1995. Interleukin 12 induces tyrosine phosphorylation and  
503 activation of STAT4 in human lymphocytes. *Proc. Natl. Acad. Sci. U. S. A.* 92: 7307–  
504 11.
- 505 32. Dinarello, C. A., D. Novick, S. Kim, and G. Kaplanski. 2013. Interleukin-18 and IL-  
506 18 binding protein. *Front. Immunol.* 4: 1–10.
- 507 33. So, T., and M. Croft. 2012. Regulation of the PKC $\theta$ -NF- $\kappa$ B axis int lymphocytes by  
508 the tumor necrosis factor receptor family member OX40. *Front. Immunol.* 3: 1–8.
- 509 34. Rex, D. A. B., N. Agarwal, T. S. K. Prasad, R. K. Kandasamy, Y. Subbannayya, and  
510 S. M. Pinto. 2020. A comprehensive pathway map of IL-18-mediated signalling. *J. Cell*  
511 *Commun. Signal.* 14: 257–266.
- 512 35. Kim, J. H., T. G. Choi, S. Park, H. R. Yun, N. N. Y. Nguyen, Y. H. Jo, M. Jang, J.  
513 Kim, J. Kim, I. Kang, J. Ha, M. P. Murphy, D. G. Tang, and S. S. Kim. 2018.  
514 Mitochondrial ROS-derived PTEN oxidation activates PI3K pathway for mTOR-  
515 induced myogenic autophagy. *Cell Death Differ.* 25: 1921–1937.
- 516 36. Singer, G. G., A. C. Carrera, A. Marshak-Rothstein, C. Martinez, and A. K. Abbas.  
517 1994. Apoptosis, Fas and systemic autoimmunity: the MRL-lpr/lpr model. *Curr Opin*  
518 *Immunol* 6: 913–920.
- 519 37. Walker, L. S., and A. K. Abbas. 2002. The enemy within: keeping self-reactive T  
520 cells at bay in the periphery. *Nat Rev Immunol* 2: 11–19.
- 521 38. Murphy, M. P., and R. M. Siegel. 2013. Mitochondrial ROS fire up T cell

- 522 activation. *Immunity* 38: 201–2.
- 523 39. Akkaya, B., A. S. Roesler, P. Miozzo, B. P. Theall, J. Al Souz, M. G. Smelkinson, J.  
524 Kabat, J. Traba, M. N. Sack, J. A. Brzostowski, M. Pena, D. W. Dorward, S. K. Pierce,  
525 and M. Akkaya. 2018. Increased Mitochondrial Biogenesis and Reactive Oxygen  
526 Species Production Accompany Prolonged CD4 + T Cell Activation . *J. Immunol.* 201:  
527 3294–3306.
- 528 40. Van Der Windt, G. J. W., D. O’Sullivan, B. Everts, S. C. C. Huang, M. D. Buck, J.  
529 D. Curtis, C. H. Chang, A. M. Smith, T. Ai, B. Faubert, R. G. Jones, E. J. Pearce, and E.  
530 L. Pearce. 2013. CD8 memory T cells have a bioenergetic advantage that underlies their  
531 rapid recall ability. *Proc. Natl. Acad. Sci. U. S. A.* 110: 14336–14341.
- 532 41. Hoth, M., D. C. Button, and R. S. Lewis. 2000. Mitochondrial control of calcium-  
533 channel gating: A mechanism for sustained signaling and transcriptional activation in T  
534 lymphocytes. *Proc. Natl. Acad. Sci.* 97: 10607–10612.
- 535 42. Potla, R., T. Koeck, J. Wegrzyn, S. Cherukuri, K. Shimoda, D. P. Baker, J.  
536 Wolfman, S. M. Planchon, C. Esposito, B. Hoit, J. Dulak, A. Wolfman, D. Stuehr, and  
537 A. C. Lerner. 2006. Tyk2 tyrosine kinase expression is required for the maintenance of  
538 mitochondrial respiration in primary pro-B lymphocytes. *Mol. Cell. Biol.* 26: 8562–  
539 8571.
- 540 43. Rieux-Laucat, F., F. Le Deist, C. Hivroz, I. A. Roberts, K. M. Debatin, A. Fischer,  
541 and J. P. de Villartay. 1995. Mutations in Fas associated with human  
542 lymphoproliferative syndrome and autoimmunity. *Science* 268: 1347–1349.
- 543 44. Balomenos, D., R. Shokri, L. Daszkiewicz, C. Vázquez-Mateo, and C. Martínez-A.  
544 2017. On How Fas Apoptosis-Independent Pathways Drive T Cell Hyperproliferation  
545 and Lymphadenopathy in lpr Mice. *Front. Immunol.* 8.  
546

547 **Abbreviations used in this article:**

548 AICD: activation-induced cell death

549 ALPS: autoimmune lympho-proliferative syndrome

550 ConA: concavalin A

551 DPI: diphenyleneiodonium

552 ETC: electron transport chain

553 FCCP: carbonyl cyanide 4-(trifluoromethoxy)phenylhydrazone

554 IRAK: interleukin 1 receptor-associated kinase

555 MFI: median fluorescence intensity

556 mROS: mitochondrial reactive oxygen species

557 Nox: NADPH oxidase

558 TMRM: tetramethylrhodamine, methyl ester, perchlorate

559 TRAF6: TNF receptor-associated factor 6

560 WT: wild-type

561 **Figure legends**

562 **Figure 1. IFN- $\gamma$  production and mROS levels in memory vs. naïve CD4<sup>+</sup> T cells.**

563 Naïve CD4<sup>+</sup> T cells were isolated from WT mouse spleens and stimulated with ConA or  
564 IL-12 and IL-18. To generate memory T cells, ConA-stimulated CD4<sup>+</sup> cells were  
565 expanded in IL-2 for 6 days and re-stimulated with either ConA or IL-12 and IL-18. (A)  
566 Flow cytometry analysis of the intracellular staining showing the percentage of IFN- $\gamma$ -  
567 producing CD4<sup>+</sup> naïve and memory T cells after 24 h stimulation with ConA or IL-12  
568 and IL-18. (B) Flow cytometry analysis of mitoSOX red fluorescence showing the  
569 percentage of mitoSOX<sup>hi</sup> cells in naïve and memory cells at 1 hour after ConA or IL-12  
570 and IL-18 stimulation. The graphs show mean  $\pm$  SD ( $n = 3$ ), \* $p < 0.05$ , \*\* $p < 0.01$ ,  
571 \*\*\* $p < 0.001$ , \*\*\*\* $p < 0.0001$ , 2-way ANOVA (with Sidak's correction for multiple  
572 comparison).

573 **Figure 2. DPI treatment lowers mROS levels and inhibits IFN- $\gamma$  production**

574 **induced by IL-12 plus IL-18 in naïve CD4<sup>+</sup> T cells.** Naïve CD4<sup>+</sup> T cells from WT  
575 mouse spleens were stimulated with IL-12 and IL-18 and analyzed by flow cytometry.  
576 (A) MitoSOX red fluorescence staining showing mROS induction at early time points  
577 after IL-12 plus IL-18 stimulation, and its reduction by DPI treatment. Gated on  
578 mitoSOX<sup>hi</sup> population. (B) Intracellular staining showing the frequency of IFN- $\gamma$ -  
579 producing CD44<sup>hi</sup> cells after 24 h of IL-12 plus IL-18 stimulation, and its reduction by  
580 DPI treatment. Gated on CD4<sup>+</sup> cells. (C) Similar surface expression of CD44 activation  
581 marker in control and DPI-treated cells after 24 h of IL-12 plus IL-18 stimulation.  
582 Histograms and dot-plots are representative of at least 3 experiments performed. Graphs  
583 show mean  $\pm$  SD ( $n=3$ ); \* $p < 0.05$ ; \*\*\* $p < 0.001$ ; \*\*\*\* $p < 0.0001$ ; two-way ANOVA with  
584 Sidak's correction; # compared to 0 time point, \* DPI treatment compared to control

585 (A); one-way ANOVA with post-hoc Tukey test (B) and (C). *n* represents values  
586 obtained from different mice.

587 **Figure 3. DPI treatment lowers mROS levels and inhibits IFN- $\gamma$  production in**  
588 **differentiated memory-like CD4<sup>+</sup> T cells.** CD4<sup>+</sup> T cells from WT mouse spleens were  
589 stimulated with ConA for 24 h, expanded in the presence of IL2 for 6 days, and  
590 stimulated with IL-12 and IL-18. (A) mitoSOX red fluorescence showing increased  
591 mROS production in the early time points of IL-12/IL-18 stimulation, and its reduction  
592 after DPI treatment. (B) Intracellular staining showing reduced frequency of IFN- $\gamma$ -  
593 producing CD44<sup>hi</sup> effector/memory T cells after DPI treatment; gated on CD4<sup>+</sup> cells.  
594 (C) Flow cytometry analysis showing decreased surface expression of CD44 after DPI  
595 treatment. Dot plots and histograms are representative of at least 3 experiments  
596 performed. Graphs show mean  $\pm$  SD (*n*=3); \**p*<0.05; \*\**p*<0.01; \*\*\**p*<0.001;  
597 \*\*\*\**p*<0.0001, two-way ANOVA with Sidak's correction; # compared to 0 time point,  
598 \* DPI treatment compared to control (A); one-way ANOVA with post-hoc Tukey test  
599 (B) and (C). *n* represents values obtained from different mice.

600 **Figure 4. The effect of different respiratory chain blockers on mROS generation,**  
601 **IFN- $\gamma$  production and mitochondrial membrane potential.** CD4<sup>+</sup> T cells from WT  
602 mouse spleens were stimulated with ConA for 24 h, expanded in the presence of IL2 for  
603 6 days, and stimulated with IL-12 and IL-18. (A) mROS production in mitoSOX<sup>hi</sup>  
604 population was unaffected by antimycin A and reduced by rotenone treatment. (B) Flow  
605 cytometry analysis showing the percentages of IFN- $\gamma$ -producing and CD44<sup>hi</sup> cells after  
606 antimycin A and rotenone treatment; gated on CD4<sup>+</sup> cells. (C) DPI treatment did not  
607 affect mitochondrial membrane potential at early time points post IL-12 plus IL-18  
608 treatment, as shown by TMRM fluorescence measured by flow cytometry. FCCP was

609 used to depolarize the membrane and show background staining (not shown). Graphs  
610 show mean  $\pm$  SD ( $n=3$ ); \* $p<0.05$ ; \*\* $p<0.01$ ; \*\*\* $p<0.001$ ; \*\*\*\* $p<0.0001$ , two-way  
611 ANOVA with Sidak's correction (A) and (C); one-way ANOVA with post-hoc Tukey  
612 test (B).  $n$  represents values obtained from different mice.

613 **Figure 5. The effect of different inhibitors on signaling pathways triggered by IL-**  
614 **12 and IL-18.** CD4<sup>+</sup> T cells from WT mouse spleens were stimulated with ConA for 24  
615 h, expanded in the presence of IL2 for 6 days, and stimulated with IL-12 and IL-18.  
616 Immunoblot analysis showing I $\kappa$ B $\alpha$  and p-PKC- $\theta$  and levels after DPI (A) and rotenone  
617 (B) treatment. (C) EMSA analysis showing reduced NF- $\kappa$ B nuclear activity after DPI  
618 and rotenone treatment. (D) Immunoblot analysis of STAT4 and AKT phosphorylation  
619 after NAC, rotenone and DPI treatment.  $\beta$ -actin was used as loading control. Shown are  
620 representative gels of at least 2 experiments performed.

621 **Figure 6. mROS drives increased IFN- $\gamma$  production in *lpr* CD44<sup>hi</sup>CD62L<sup>lo</sup>CD4<sup>+</sup> T**  
622 **cells.** CD4<sup>+</sup> T cells from WT and *lpr* mouse spleens were stimulated with ConA for 24  
623 h, expanded in presence of IL-2 for 6 days and stimulated with IL-12 and IL-18. (A)  
624 Flow cytometry analysis showing increased mROS production in mitoSOX<sup>hi</sup> *lpr* cells  
625 compared with WT at 60 min after IL-12 plus IL-18 stimulation. (B) The effect of DPI  
626 treatment on mROS production by WT and *lpr* cells at 60 min after IL-12 plus IL-18  
627 stimulation. (C) Flow cytometry analysis showing unaffected CD44 surface expression  
628 in WT and *lpr* cells after IL-12 plus IL-18 treatment. (D) Intracellular staining showing  
629 increased frequency of IFN- $\gamma$ -producing CD44<sup>hi</sup> *lpr* cells compared with WT and their  
630 reduction after DPI treatment. (E) Flow cytometry analysis of CD62L and CD44  
631 surface expression showing the increased proportions of *lpr* CD44<sup>hi</sup>CD62L<sup>lo</sup> cells  
632 compared with WT and their reduction after DPI treatment. Shown are representative

633 dot plots of 3 experiments performed. Graphs show mean  $\pm$  SD ( $n=3$ );  $*p<0.05$ ;

634  $**p<0.01$ ;  $***p<0.001$ ;  $****p<0.0001$ , two-way ANOVA with Sidak's correction.  $n$

635 represents values obtained from different mice.



Figure 1

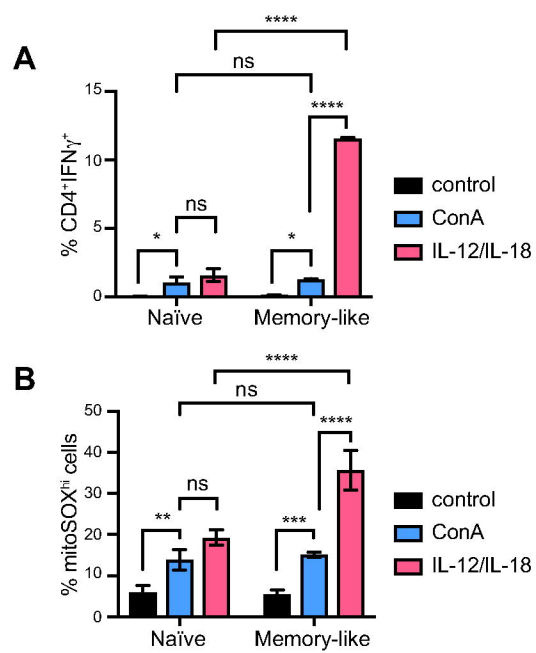


Figure 2

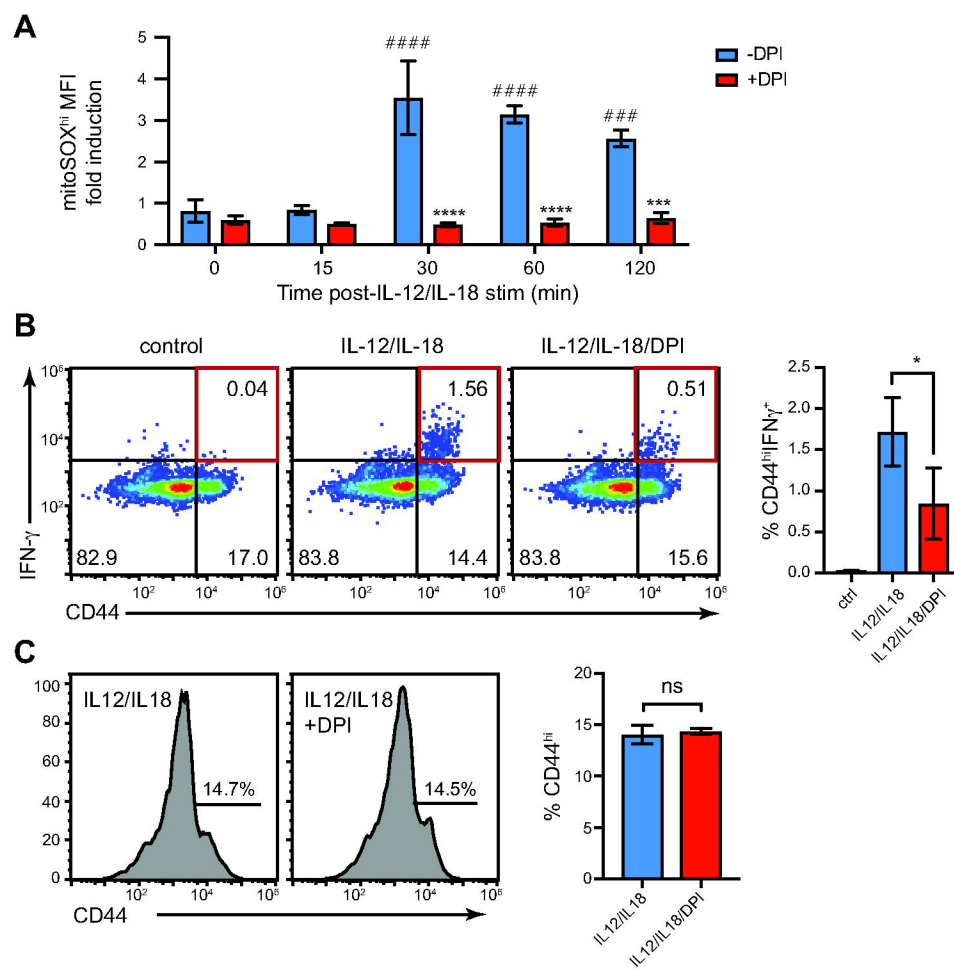


Figure 3

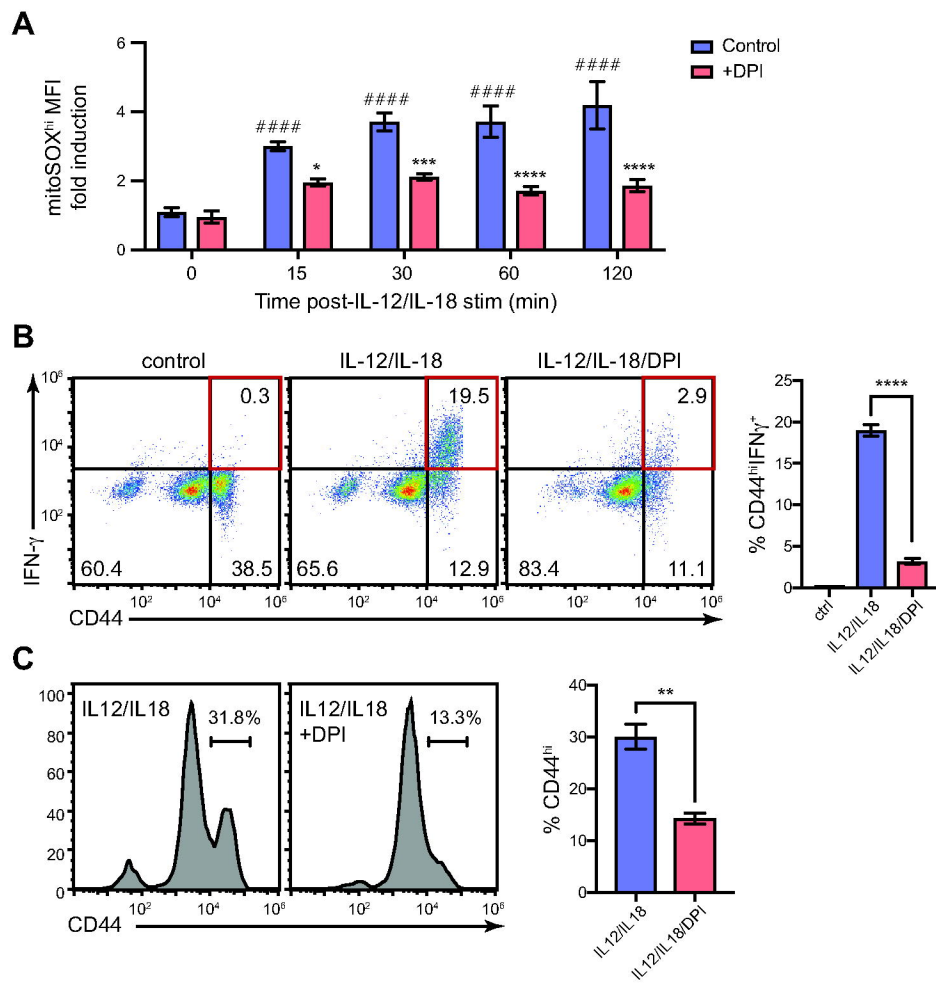
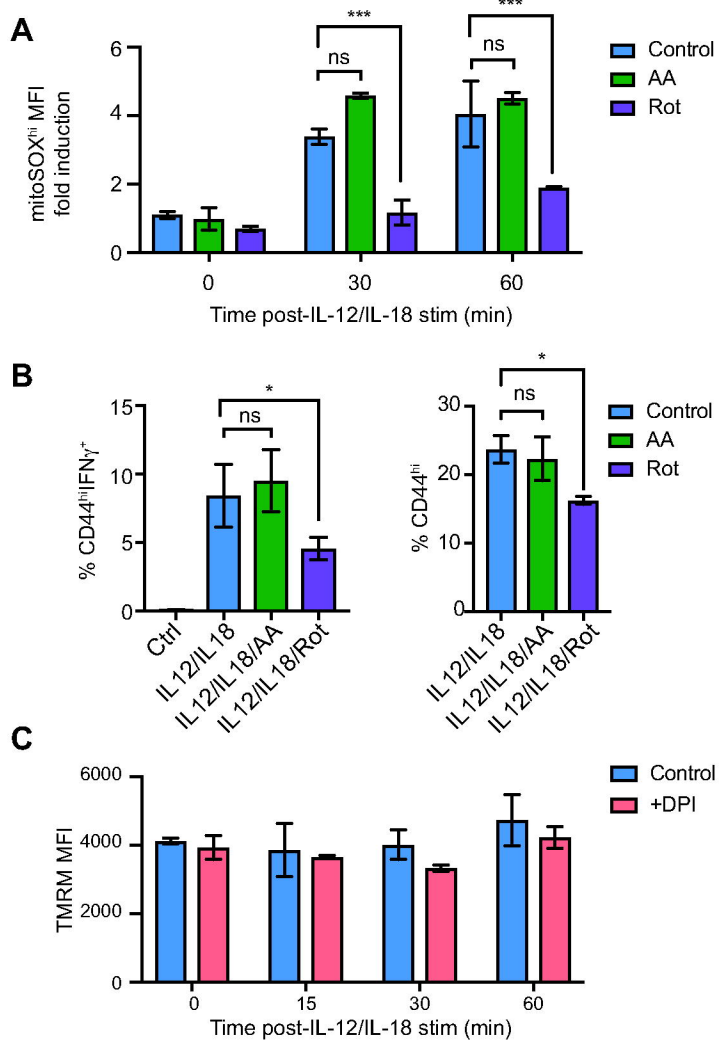
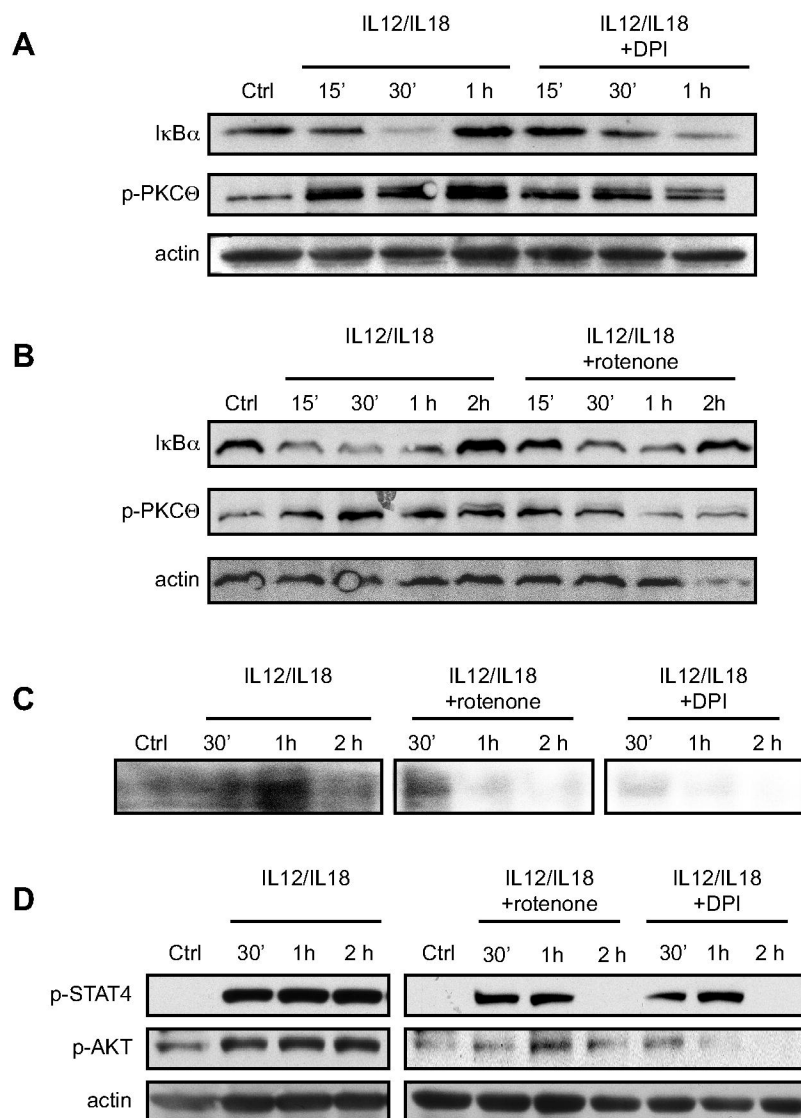


Figure 4



## Figure 5



**Figure 6**

